

# Development of comprehensive temperature-dependent plasma-chemical kinetic reaction mechanisms for plasma systems at elevated temperatures (300–1200 K)

R. Snoeckx<sup>1</sup> and M. S. Cha<sup>1</sup>

<sup>1</sup>CCRC, Physical Science and Engineering (PSE) Division, King Abdullah University of Science and Engineering (KAUST), Thuwal 23955, Saudi Arabia

**Abstract:** Non-thermal plasma discharges could play an important role in supporting and/or electrifying traditional thermal processes. To scientifically advance applications in this area, plasma-chemical kinetic studies must describe both electron-induced and thermally-induced reactions. Here we present our effort to establish a combined experimental and modelling platform, and the development of a temperature-dependent H<sub>2</sub>/O<sub>2</sub> plasma-chemical reaction mechanism as building block to study any temperature-dependent plasma-assisted process.

**Keywords:** H<sub>2</sub>, O<sub>2</sub>, HO<sub>2</sub>, plasma-chemical kinetics, temperature-controlled DBD.

## 1. Introduction

Plasma processes have the potential to become a key technology for transforming electrical energy into chemical energy by synthesizing chemicals and fuels of interest. Additionally, as the production of energy is shifting to renewable sources, a similar shift towards electrification in industrial processes is on the horizon.[1]

While one of the main strengths of plasmas is initiating reactions through electron collisions leading to the production of radicals, the selective recombination of these radicals to desired products remains challenging. Recently, we revealed that although electron-induced reactions initiate chemical reactions regardless of temperature, the thermally induced reactions have a dominant effect on the selectivity and final product composition.[1-4]

A promising route to affect the process selectivity is the combination of plasma with a catalyst. This approach can increase selectivity and yield, and decrease the temperature requirements. The plasma-catalyst interaction highly depends on the process, the plasma properties and the type of catalyst. The catalyst can be activated by a combination of heat and the plasma generated reactive species.[5]

As a result plasma technology provides unique possibilities by providing two independent ways to control chemical reactions: electron-induced and thermally induced chemistry. This also highlights the need to explore the effect of the gas temperature on processes of interest for non-thermal plasma discharges.

To date, most work has focused either on the development of room temperature plasma-chemical reaction mechanisms or temperature-dependent plasma-chemical reaction mechanisms under highly diluted conditions. However, due to the differences in system reactivity, extending these studies to realistic conditions (e.g., practically diluted atmospheric or higher pressures) is not without complications.[6-7]

Therefore, we developed a combined experimental and modelling approach, and compiled a temperature-dependent plasma-chemical reaction mechanism for gas temperatures below 1200 K to study any temperature-

dependent plasma-assisted process (oxidation, reduction, combustion, reforming, synthesis, catalysis). Here we introduce our modelling approach and present the results for the first step, a H<sub>2</sub>/O<sub>2</sub> plasma-chemical reaction mechanism which serves as a building block for both carbon (CO<sub>2</sub>, [8] CH<sub>4</sub>, higher hydrocarbons, alcohols) and nitrogen (N<sub>2</sub>, NO<sub>x</sub>, NH<sub>3</sub> [9-10]) containing systems.

Interestingly, even for a simple H<sub>2</sub>/O<sub>2</sub> mixture, a non-linear temperature-dependent trend in the form of Negative Temperature Coefficient (NTC)-like behavior was experimentally observed in a temperature range of 575–775 K. Based on numerical analyses, this NTC behavior could be attributed to a combination of the electron-induced and thermally induced chemistry.

## 2. Description of the model

### 2.1. KAUSTKin

We developed a zero-dimensional (0D) plasma-chemical kinetic model, KAUSTKin.[11] The model couples ZDPlasKin [12] and Chemkin [13] to solve the time-dependent species and energy equations. The rates of electron impact reactions are calculated in ZDPlasKin using the Boltzmann equation solver (BOLSIG+ [14]) based on the supplied cross-section data and the corresponding electron energy distribution function (EEDF). The rates of the conventional (thermal) reactions, on the other hand, are calculated by the Chemkin library. A schematic representation of the model is given in **Figure 1**, more details about KAUSTKin can be found in [11].

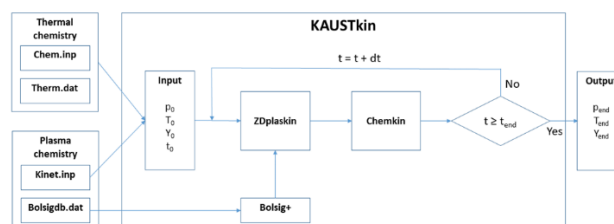


Fig. 1. Schematic of the modules and data flow of the plasma-chemical kinetic model, KAUSTKin. Reproduced from ref [11] with kind permission; published by Elsevier.

## 2.2. Temperature-dependent reaction mechanism

The reaction mechanism shown here consists of three parts: a plasma H<sub>2</sub>/O<sub>2</sub> mechanism for the electron-induced chemistry, a conventional (thermal) H<sub>2</sub>/O<sub>2</sub> mechanism, and an ozone (O<sub>3</sub>) mechanism.

The plasma H<sub>2</sub>/O<sub>2</sub> mechanism was compiled from literature consisting of 265 reactions with electrons, ions, and excited species, and relied on the Biagi database [15] for electron impact cross section data.

For the conventional thermal H<sub>2</sub>/O<sub>2</sub> mechanism we started from NUIGMech1.1 (35 reversible reactions), [16-17] and modified it by (i) replacing the rate data for H + HO<sub>2</sub> → H<sub>2</sub> + O<sub>2</sub> with the data from Konnov, [18-19] (ii) replacing the rate data for H + O<sub>2</sub> (+M) → HO<sub>2</sub> + M, [20] and (iii) adding eight reversible O<sub>3</sub> reactions. [11] As a result, the full mechanism considered 21 species (**Table 1**) and 351 reactions: 155 electron impact reactions, 14 ion reactions, 112 reactions with excited states, and 70 neutral reactions.

The plasma mechanism omitted several electronic and vibrational excited states and parts of the ion-ion chemistry, maintaining minimal electron-ion reactions (see [11]). This approach greatly reduced the complexity of the mechanism and analysis, so that the mechanism can be further optimized for multi-dimensional simulations in the future.

Table 1. Species included in the temperature-dependent H<sub>2</sub>/O<sub>2</sub> plasma-chemical reaction mechanism.

	Neutral	Excited	Charged
<b>electrons</b>			e <sup>-</sup>
<b>O containing</b>	O <sub>3</sub> O <sub>2</sub> O	O <sub>2</sub> (a <sup>1</sup> ), O <sub>2</sub> (b <sup>1</sup> ), O <sub>2</sub> (c) O( <sup>1</sup> D), O( <sup>1</sup> S)	O <sub>2</sub> <sup>+</sup> O <sup>+</sup>
<b>H containing</b>	H <sub>2</sub> H		H <sub>2</sub> <sup>+</sup> H <sup>+</sup>
<b>O-H containing</b>	OH HO <sub>2</sub> H <sub>2</sub> O H <sub>2</sub> O <sub>2</sub>	OH(V)	H <sub>2</sub> O <sup>+</sup>

## 3. Description of the experiments

The experimental apparatus consisted of a temperature-controlled dielectric barrier discharge (DBD) reactor, a power supply system, a reactant supply system, and an analysis system. The temperature-controlled DBD reactor was composed of an electric furnace containing a coaxial DBD reactor consisting of a quartz tube with an inner diameter of 20-mm, and a stainless-steel rod with a diameter of 18-mm serving as high voltage electrode, resulting in a 1-mm discharge gap. A 40-mm wide stainless-steel mesh was wrapped around the outside of the quartz tube to serve as a ground electrode (**Figure 2**). H<sub>2</sub> (Parker, 40H, hydrogen generator, 99.99995 %) and O<sub>2</sub> (99.995 %) were used as feed gases with a constant total flow rate of 200 sccm. The reactor was supplied by an adjustable high voltage AC power supply (Trek), which could supply voltage and current up to 20 kV. The discharge power ( $P_{dis}$ ) was varied between 1.25–20 W,

providing a specific energy input for all investigated cases of 0.375–6 J/cm<sup>3</sup>. The gas temperature ( $T_g$ ) was varied between 300–900 K. The analysis system consisted of an inline gas chromatograph (GC) with two calibrated Thermal Conductivity Detectors (TCD), which were used to analyze the conversion of O<sub>2</sub> and H<sub>2</sub> as a measure for the oxidation of H<sub>2</sub>. More details about the experimental setup can be found in [11].

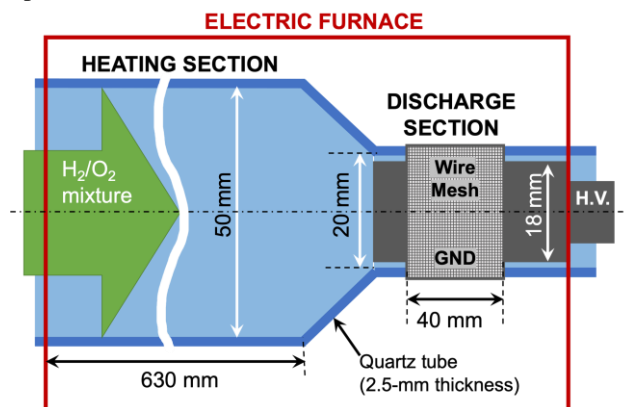


Fig. 2. Schematic of the experimental setup. Reproduced from ref [11] with kind permission; published by Elsevier.

## 4. Results and discussion

To validate the temperature-dependent plasma-chemical H<sub>2</sub>/O<sub>2</sub> reaction mechanism, the oxidation of H<sub>2</sub> was studied for three different mixtures: extremely lean ( $\phi = 0.01$ , **Figure 3a**), extremely rich ( $\phi = 49.5$ , **Figure 3b**), and stoichiometric ( $\phi = 1$ , **Figure 3c**). This approach allowed to separately evaluate the effects of the O<sub>2</sub> chemistry, the H<sub>2</sub> chemistry, and its combination, respectively.

For all mixtures non-linear NTC-like oxidation behaviour was observed in a temperature range of  $575 \leq T_g \leq 775$  K. This behavior could be attributed to a combination of physical and chemical effects: (i) the dominant contribution originated from non-linear changes to the reduced electric field ( $E/N$ ) as  $T_g$  was varied in the DBD reactor, which affected the degree of energy transferred to the electron-impact dissociation processes; and (ii) the OH production was influenced by the temperature-dependent kinetics related with H and HO<sub>2</sub>, showing similar behaviour compared to conventional NTC-kinetics with saturated hydrocarbons. Based on chemical and sensitivity analyses HO<sub>2</sub> was found to be the most important intermediate species governing the overall oxidation process, however, the key reactions responsible for the NTC behavior varied for the different mixtures.

### 4.1. Extremely lean ( $\phi = 0.01$ )

For the extremely lean case (98 vol% O<sub>2</sub> and 2 vol% H<sub>2</sub>, **Figure 3a**) the oxidation process is initiated by the electron impact dissociation of O<sub>2</sub> to form O and O(<sup>1</sup>D) radicals, whereas the electron impact dissociation of H<sub>2</sub> is insignificant. This is in stark contrasts with the result of highly diluted mixtures, where excited metastable states of the diluent (such as Ar or He) dominate the dissociation of O<sub>2</sub> and H<sub>2</sub> through dissociative quenching reactions [7].

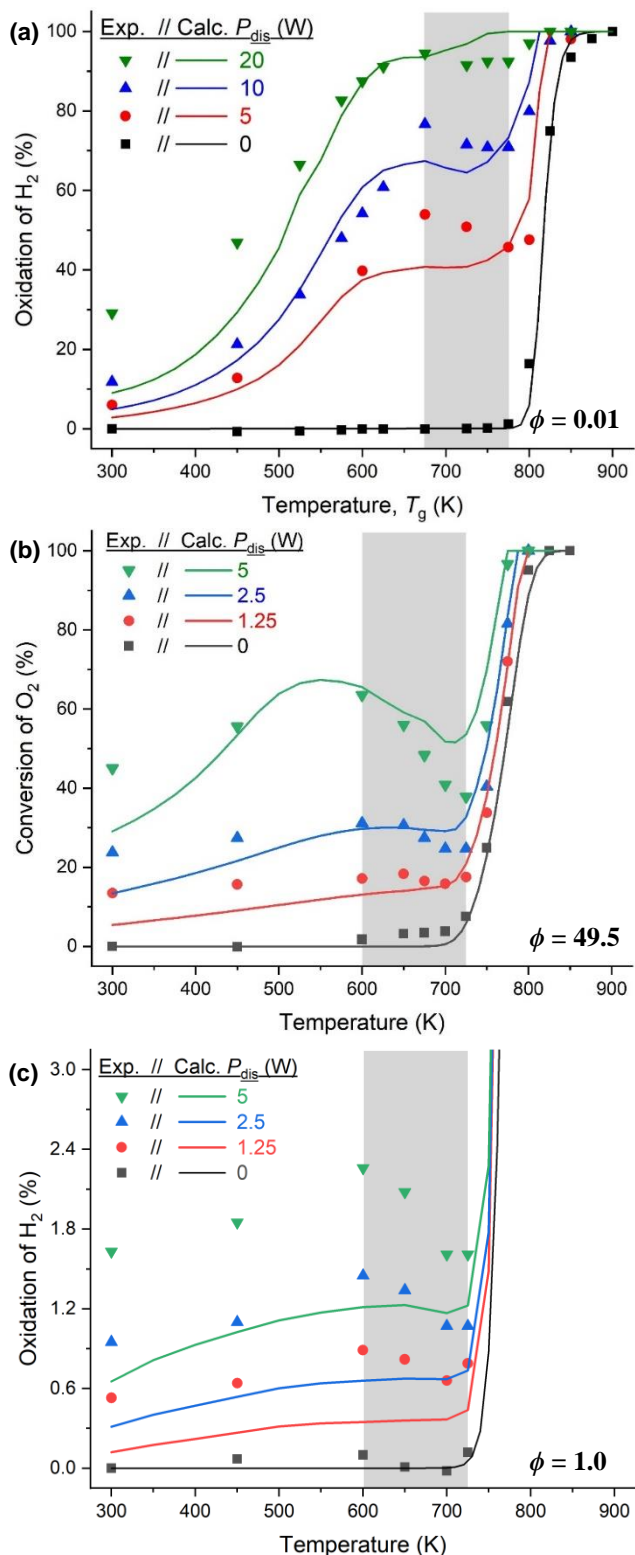


Fig. 3. Experimental (symbols) and numerical (solid lines) results for the plasma-assisted oxidation of H<sub>2</sub>/conversion of O<sub>2</sub> as a function of T<sub>g</sub> for the H<sub>2</sub>/O<sub>2</sub> mixture ( $\phi$  = (a) 0.01, (b) 49.5, and (c) 1.0) at various P<sub>dis</sub>. The grey shaded area indicates the experimentally found NTC-like regime.

At  $T_g < 575$  K O(<sup>1</sup>D) was mainly responsible for the seed of H radicals ( $O(^1D) + H_2 \rightarrow OH + H$  (R1)), which are required to produce the key intermediate, HO<sub>2</sub>. The HO<sub>2</sub> pathway transformed H radicals into OH radicals via  $H + O_2 (+M) \rightarrow HO_2 (+M)$  (R2) and  $HO_2 + O \rightarrow OH + O_2$  (R3).

However, at this T<sub>g</sub>, O<sub>3</sub> production suppresses the oxidation reactions R1 and R3 by consuming the available O radicals ( $O + O_2 (+M) \rightarrow O_3 (+M)$  (R4)) and OH radicals ( $O_3 + OH \rightarrow O_2 + HO_2$  (R5)).

At  $575 \leq T_g \leq 700$  K, a transition of reactions occurs: (i) a gradual shift in the main branching and propagation reactions producing OH towards  $H_2 + O \rightarrow OH + H$  (R6), (ii) a high HO<sub>2</sub> production in combination with the chain termination reaction,  $HO_2 + HO_2 \rightarrow H_2O_2 + O_2$  (R7), leads to a deteriorated OH production rate, resulting in NTC-like behavior.

At  $T_g \geq 700$  K, consumption of HO<sub>2</sub> occurs via  $H + HO_2 \rightarrow OH + OH$  (R8), which together with increased rates of the chain branching reactions  $H_2 + O \rightarrow OH + H$  (R9) and especially  $O_2 + H \rightarrow O + OH$  (R10) leads to the recovery of the OH production and hence oxidation process.

Interestingly, the excited states of O-species (mainly transferring energy through collisional quenching) played a minor role in the overall oxidation process.

#### 4.2. Extremely rich ( $\phi = 49.5$ )

For the extremely rich case (1 vol% O<sub>2</sub> and 99 vol% H<sub>2</sub>, **Figure 3b**) the oxidation process is initiated by the electron impact dissociation of H<sub>2</sub>, to form H radicals, whereas the electron impact dissociation of O<sub>2</sub> is negligible. To obtain similar oxidation P<sub>dis</sub> was lowered by a factor of four, due to the enriched chain branching reactions and the absence of oxidation limiting O<sub>3</sub> production in the rich mixture.

Again, HO<sub>2</sub> was the key species controlling the oxidation process through the transformation of H radicals into OH radicals via R2 and R8, eventually leading to full oxidation through  $H_2 + OH \rightarrow H_2O + H$  (R11).

At  $T_g < 575$  K, H<sub>2</sub>O<sub>2</sub> production slightly suppressed the oxidation by consuming both HO<sub>2</sub> radicals via R7 and OH radicals via  $H_2O_2 + OH \rightarrow H_2O + HO_2$  (R12).

At  $575 \leq T_g \leq 700$  K, a significant increase in the chain termination reaction  $H + HO_2 \rightarrow H_2 + O_2$  (R13) led to: (i) a gradual decrease in the production of HO<sub>2</sub> via R2, and (ii) gradual decrease in the production of OH via R8, due to the competition for the available H and HO<sub>2</sub> radicals, which again leads to a deteriorated OH production rate, resulting in NTC-like behavior.

At  $T_g \geq 700$  K, increased rates of the chain branching reactions R9 and especially R10 leads to the recovery of the OH production and hence oxidation process.

#### 4.3. Stoichiometric ( $\phi = 1$ )

For the stoichiometric case (33.3 vol% O<sub>2</sub> and 66.7 vol% H<sub>2</sub>, **Figure 3c**) the oxidation process is initiated by a combination of the electron impact dissociation of H<sub>2</sub> and O<sub>2</sub>, leading to the production of H, O and O(<sup>1</sup>D) radicals.

HO<sub>2</sub> remained the key species controlling the oxidation process through the transformation of H radicals into OH

radicals via R2 and R8, followed by full oxidation through R11. From the chemical and sensitivity analyses it became clear that the observed oxidation behaviour for the stoichiometric case, is governed by a combination of the mechanisms observed for both the lean and rich cases. Additionally, the high H radical and O<sub>2</sub> concentration leads to a significant production of HO<sub>2</sub> (R2) and H<sub>2</sub>O<sub>2</sub> (R7).

Based on the high uncertainty and the high sensitivity of the oxidation process to reactions R2, R8, and R13, these are considered as key reactions to further optimizations of the H<sub>2</sub>/O<sub>2</sub> reaction mechanisms.

## 5. Conclusions

We developed a combined experimental and modelling platform, and compiled a temperature-dependent H<sub>2</sub>/O<sub>2</sub> plasma-chemical reaction mechanism for gas temperatures below 1200 K as building block to study any temperature-dependent plasma-assisted process (oxidation, reduction, combustion, reforming, synthesis, catalysis).

For the first time non-linear temperature-dependent oxidation behavior in the form of a NTC-like trend was observed for a H<sub>2</sub>/O<sub>2</sub> mixture in a temperature range of 575–775 K. Through a numerical analysis this could be attributed to a combination of the electron-induced and thermally induced chemistry. As such, our findings emphasized the significance of both plasma-physical characteristics and plasma-chemical kinetics on temperature-dependent plasma-assisted processes.

Future efforts should continue in this direction, focusing on rigorous, fundamental investigations into temperature-dependent plasma-chemical kinetics, with as final goal to design and develop plasma systems for any target process. Special attention in this area should be given to the production of carbon-free fuels such as H<sub>2</sub> and NH<sub>3</sub>, and the production of feedstock (petro)chemicals.

## 6. Acknowledgements

The authors acknowledge financial support from King Abdullah University of Science and Technology (KAUST), under award number BAS/1/1384-01-01.

## 7. References

[1] M. S. Cha and R. Snoeckx, "Plasma Technology—Preparing for the Electrified Future," *Front. Mech. Eng.*, **8**, 1 (2022).

[2] X. Zhang and M. S. Cha, "Electron-induced dry reforming of methane in a temperature-controlled dielectric barrier discharge reactor," *J. Phys. D. Appl. Phys.*, **46**, 415205 (2013).

[3] X. Zhang and M. S. Cha, "Partial oxidation of methane in a temperature-controlled dielectric barrier discharge reactor," *Proc. Combust. Inst.*, **35**, 3447 (2015).

[4] J.-L. Liu, R. Snoeckx, and M. S. Cha, "Steam reforming of methane in a temperature-controlled dielectric barrier discharge reactor: the role of electron-induced chemistry versus thermochemistry," *J. Phys. D. Appl. Phys.*, **51**, 385201 (2018).

[5] E. C. Neyts, K. Ostrikov, M. K. Sunkara, and A. Bogaerts, "Plasma Catalysis: Synergistic Effects at the Nanoscale," *Chem. Rev.*, **115**, 13408 (2015).

[6] W. Wang, R. Snoeckx, X. Zhang, M. S. Cha, and A. Bogaerts, "Modeling Plasma-based CO<sub>2</sub> and CH<sub>4</sub> Conversion in Mixtures with N<sub>2</sub>, O<sub>2</sub>, and H<sub>2</sub>O: The Bigger Plasma Chemistry Picture," *J. Phys. Chem. C*, **122**, 8704 (2018).

[7] R. Snoeckx and M. S. Cha, "Inevitable chemical effect of balance gas in low temperature plasma assisted combustion," *Combust. Flame*, **225**, 1, (2021).

[8] A. Mohanan, S. Bang, R. Snoeckx, and M. S. Cha, "Carbon dioxide: A Study into Temperature-dependent Carbon-based Plasma Chemistry," *ISPC-25* (2023).

[9] S. Bang, R. Snoeckx, and M. S. Cha, "A combined experimental and modelling study for the development of a plasma-chemical kinetic reaction mechanism for NH<sub>3</sub> cracking," *ISPC-25* (2023).

[10] S. Bang, R. Snoeckx, and M. S. Cha, "Kinetic Study for Plasma Assisted Cracking of NH<sub>3</sub>: Approaches and Challenges," *J. Phys. Chem. A*, in press (2023).

[11] R. Snoeckx, D. Jun, B. J. Lee, and M. S. Cha, "Kinetic study of plasma assisted oxidation of H<sub>2</sub> for an undiluted lean mixture," *Combust. Flame*, **242**, 112205 (2022).

[12] S. Pancheshnyi, B. Eismann, G. J. M. Hagelaar, and L. C. Pitchford, "ZDPlasKin: a new tool for plasmachemical simulations." (2008).

[13] R. Kee, F. Rupley, and J. Miller, "Chemkin-II: A Fortran chemical kinetics package for the analysis of gas-phase chemical kinetics," (1989).

[14] G. J. M. Hagelaar and L. C. Pitchford, "Solving the Boltzmann equation to obtain electron transport coefficients and rate coefficients for fluid models," *Plasma Sources Sci. Technol.*, **14**, 722 (2005).

[15] S. F. Biagi, "Biagi database (Fortran program MAGBOLTZ)." [www.lxcat.net/Biagi](http://www.lxcat.net/Biagi)

[16] Y. Wu et al., "Understanding the antagonistic effect of methanol as a component in surrogate fuel models: A case study of methanol/n-heptane mixtures," *Combust. Flame*, **226**, 229 (2021).

[17] M. Baigmohammadi et al., "Comprehensive Experimental and Simulation Study of the Ignition Delay Time Characteristics of Binary Blended Methane, Ethane, and Ethylene over a Wide Range of Temperature, Pressure, Equivalence Ratio, and Dilution," *Energy and Fuels*, **34**, 8808 (2020).

[18] A. A. Konnov, "Remaining uncertainties in the kinetic mechanism of hydrogen combustion," *Combust. Flame*, **152**, 507 (2008).

[19] R. Snoeckx and M. Cha, "Kinetic study of plasma assisted oxidation of H<sub>2</sub> for an undiluted rich mixture," *Combust. Flame*, in press (2023).

[20] R. Snoeckx and M. Cha, "Kinetic study of plasma assisted oxidation of H<sub>2</sub> for (near) stoichiometric mixtures," in preparation (2023).